Polymer and Dye Probe Diffusion in Poly(methyl methacrylate) below the Glass Transition Studied by Forced Rayleigh Scattering

Andrey V. Veniaminov† and Hans Sillescu*

Institut für Physikalische Chemie, Johannes Gutenberg-Universität, Jakob-Welder-Weg 15, 55099 Mainz, Germany

Received August 19, 1998; Revised Manuscript Received January 4, 1999

ABSTRACT: By dissolving tracer quantities of 9,10-phenanthrenequinone (PQ) in poly(methyl methacrylate) (PMMA) it was possible to study by forced Rayleigh scattering (FRS) the tracer diffusion of the unbleached PQ as well as the photoproduct which is covalently bound to the PMMA molecules. The PMMA samples with molecular weights, M_w, of 10^3-10^5 were intermittently annealed at 80 °C for diffusion times of up to one year. From the results we conclude that polymer chain diffusion may be possible at temperatures more than 20 K below the glass transition temperature T_g, but further experiments are necessary, in particular, since we cannot exclude that our results are due to yet unexplained long time aging effects in PMMA. The translational diffusion coefficients of the unbleached PQ are enhanced by several decades in comparison with predictions from rotational correlation times that were determined by using a modified FRS technique.

Introduction

Translational diffusion in polymer melts has been studied for many years,[1,2] and the experimental results have been compared with the reptation model[3] and possible alternatives.[4] At temperatures close to the glass transition temperature T_g the diffusion of monomeric tracers was found to depend on the probe size.[5−7] Furthermore, one has observed that on approaching T_g translational diffusion becomes increasingly enhanced in comparison with rotational diffusion of the same probes and shear viscosity.[5,6] Since this enhancement becomes less with increasing probe size, one should expect that there is no enhancement for the diffusion of macromolecules. Thus, diffusion coefficients should be unmeasurably small for large chains in polymers at the glass transition temperature T_g as one can readily see by extrapolation from D values determined in the molten state using the WLF equation[8] with parameters determined from T dependent measurements of D or the shear viscosity η. For example, one obtains from literature data[9] for polystyrene (PS) with a molecular weight of $M_n = 10^5$ extrapolated values of $D < 10^{-20}$ cm^2 s^{-1} at $T_g = 100$ °C and $D < 10^{-30}$ cm^2 s^{-1} at 80 °C. When we started the present work with PMMA oligomers we obtained surprisingly large D values at $T < T_g$. This has led us to start a long time study at $T = 80$ °C well below T_g of all investigated oligomer and polymer samples.

In addition to the FRS setup of previous diffusion studies at Mainz[5] another one was used specially designed for measuring very slow processes. It is similar to the one used in St.Petersburg[10−13] for previous studies of hologram formation and probe diffusion in PMMA samples. Thus hologram recording (writing) was done with an Ar^+ ion laser at $\lambda = 488$ nm whereas a He−Ne laser at $\lambda = 633$ nm was used for hologram reconstruction (reading) in samples which were intermittently heated to the diffusion temperature and kept in the oven for periods of up to 1 year. This allows for measuring extremely small diffusion coefficients. However, if we assume $D = 10^{-19}$ cm^2 s^{-1} and a diffusion time of one year we obtain a root-mean-square (rms) displacement across the grating of $(2Dt)^{1/2} = 25$ nm which is on the order of the rms end to end distance of 22 nm of a PS chain with $M_n = 10^5$. Thus, one should expect that the initial part of the FRS decay will be nonexponential and will reflect enhanced local motions, e.g., inside the tube of the reptation model.[3] The full FRS decay can only be observed if diffusion times $t > (\Lambda/2\pi)^2/D$ are accessible. Here, $\Lambda = \lambda/(2 \sin \theta)$ is the grating distance and 2θ the crossing angle of the coherent laser beams for recording the holographic grating.[14] Due to experimental limitations (see following section), our smallest grating distance was $\Lambda = 365$ nm which results in $D > 10^{-18}$ cm^2 s^{-1} as a lower limit if the decay is followed up to times $(\Lambda/2\pi)^2/D \sim 3.3 \times 10^7$ s. The smaller D values discussed below were obtained by analyzing the "small" time regime of the FRS decay curves.

Among a number of photosensitive systems appropriate for writing the holographic gratings that consisting of 9,10-phenanthrenequinone (PQ) in poly(methyl methacrylate) (PMMA) was chosen for the experiments. The photochemistry of PQ and the mechanism of hologram recording have been described elsewhere.[11,15,16] The basic photochemical property of PQ useful for this work is its ability to photochemically bind to the PMMA macromolecules.[17] Photoinduced binding of PQ to PMMA is demonstrated in the MALDI−TOF mass spectrum shown in Figure 1, which was obtained from a sample of ∼5% PQ in PMMA after irradiation of laser light (488 nm) at 20 °C.[18] Molar mass distributions originating from PMMA and PMMA with up to four PQ units per macromolecule (Figure 1b) are obtained from a mass shift of $M_{PQ} + nM_{MMA} = 208 + n100$ between the subensembles. The mass spectrum shows no indication of cross-linking which would result in PMMA dimers, trimers, etc. This is different from the situation with other quinones such as benzoquinone and anthraquinone.[15,19]

The holographic grating obtained in a PMMA/PQ sample consists of two counterphase photoinduced sub-

† Permanent address: S. I. Vavilov State Optical Institute, 199034, St. Petersburg, Russia.

10.1021/ma981312d CCC: $18.00
Published on Web 03/05/1999

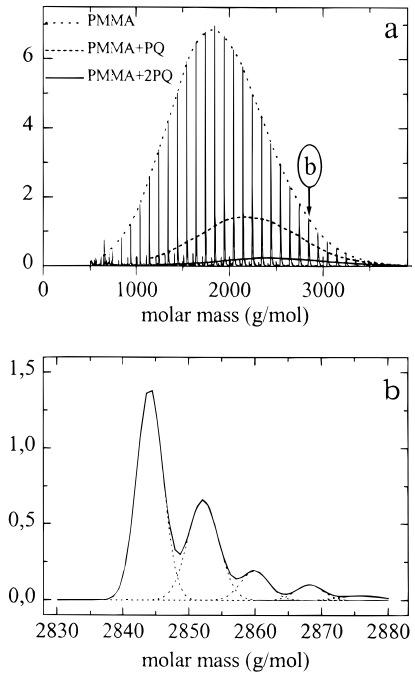

Figure 1. MALDI mass-spectrum of PMMA (M_w = 1700) sample with phenanthrenequinone molecules (5%), upon Ar^+ laser light (488 nm) exposure. (a) Full spectrum (intensity in arbitrary units). The curves show subensembles of pure PMMA macromolecules, and those photolabeled with one or two phenanthrene groups. (b) Fragment of the mass-spectrum shown above, corresponding to 28MMA (centered at 2844), 26MMA + PQ (2852), 24MMA + 2PQ (2860), 22MMA + 3PQ (2868), 20MMA + 4PQ(2876).

gratings, one built of the product of the photochemical reaction (phenanthrene chromophores chemically bound to macromolecules) and another, a complementary one, of unbleached PQ molecules.[11] As the mobility of the two species (PQ and PMMA) differs drastically due to great difference in sizes of the diffusants, one of the gratings will vanish due to PQ diffusion giving rise to an increasing diffraction efficiency, as the compensation of one grating with another weakens. The degradation of the second grating caused by diffusion of macromolecules, which is decades slower, will result in the final decay of the whole grating. This large time scale separation of two diffusion processes distinguishes the PMMA/PQ system from other systems[20,21] with complementary gratings also involved but having almost equal lifetimes. The time dependence of interference of two competing gratings finds its simplest description in terms of biexponential kinetics. For data evaluation, the exponentials will be replaced by stretched exponentials which better fit the experimental data and may somehow describe possible spatial inhomogeneity in the polymer glass. It should be noted that in this work we only deal with volume transmission-type purely phase gratings (existing due to refractive index modulation). This modulation is thus supposed to develop in time as $\Delta n(t) = A \exp[-(t/\tau_{tA})^{\beta_A}] - B \exp[-(t/\tau_{tB})^{\beta_B}]$ where $\tau_{tA,B}^{-1} = (\Lambda/2\pi)^2 D_{A,B}$. The minus sign in front of the B term is due to the phase difference, π, between the A and B gratings.

Polymer diffusion in PMMA melts has been investigated previously.[22,23] The D values obtained are as expected from diffusion studies in other polymer melts.[1,2] The diffusion of dye tracers in PMMA was also studied at temperatures down to below the glass transition temperature T_g.[5,10,13] In the present study, we have measured D values of both the PQ dye and the labeled PMMA molecules in the glass state close to T_g. In addition, we have determined the rotational correlation time of PQ and its photoproduct by following the decay of orientational order by FRS (see below[24]). This provides additional evidence for our interpretation of the results on translational diffusion.

Table 1. Characteristics of PMMA Samples

sample no.	M_w	M_w/M_n	T_g, °C (±5 °C)
1	1390	1.19	35
2	1700	1.10	65
3	4260	1.1	96
4	9110	1.24	100
5	11700	1.08	115
6	30200	1.07	117
7	35500	1.17	115
8	51700	1.23	104
9	81200	1.16	110
10	120000	6	103
11	160500	1.06	112
12	548000	1.35	105

Experimental Section

Materials and Sample Preparation. Almost all PMMA samples used in this work were synthesized according to standard techniques of anionic polymerization and group transfer polymerization[25] (see samples 1−6, 8, 9, 11, and 12 in Table 1—all predominantly syndiotactic) and they all were characterized by A. H. E. Müller and co-workers. PMMA with M_w = 35 500 was a standard produced by Polymer Laboratories LTD, U.K.; PMMA with M_w =120 000 as well as 9,10-phenanthrenequinone (purity 99+%) were purchased from Aldrich.

The samples for the previous work with PQ-based material[11,12] were prepared by bulk polymerization, which ensures good optical quality. However, the molar mass distribution is inevitably broad, and a certain concentration of residual monomer cannot be avoided. In the present paper, the samples were prepared by first freeze-drying a solution of PMMA and PQ (0.5%) in tetrahydrofurane (THF). Subsequently, the polymer−dye mixture was heated for a few minutes on a hot plate between two quartz windows, and slightly pressed until the optical homogeneity of the triplex became acceptable. To avoid thermal depolymerization, which is possible already at T > 140 °C,[26] the heating times and temperatures were kept as low as possible (80 °C for M_w < 2000, 110 °C for $M_w \lesssim$ 60 000, 150 °C for M_w = 160 500, and 160 °C for M_w = 548 000). Absence of noticeable thermal depolymerization was checked by GPC. In some cases, the polymer−dye mixture was obtained by film casting from solution and heating under vacuum, followed by the same procedure of pressing between the windows. The thickness of the samples was within the range of 0.2−0.5 mm. All samples were annealed at 80−100 °C during a few days, except for some cases of low molar weight PMMA which show particular "aging" phenomena at long annealing times (see below). Samples 1−3 ($M_w \leq$ 4260) were also kept in the metal sample holder until the diffusion experiments were completed whereas the other samples were removed and handled in the form of "sandwiches" between quartz plates during the further experiments.

Optical Setup. Two different setups were used for diffusion times up to a few hours ("fast" measurements) and up to many months ("slow" measurements), respectively. In both setups, polarized light (488 nm) of an Ar^+ ion laser (Coherent Innova 90) was used for writing the gratings. Reconstruction (reading) was done with a He−Ne laser (Polytek or Uniphase). Since neither PQ nor its photoproduct absorb light at 633 nm the diffraction efficiency results from pure phase gratings and can be very high,[11] and also attenuation of the reconstruction beam was unnecessary. Hence, the diffracted light appeared sufficient to be reliably detected by ordinary active photodiodes (Spindler & Hoyer E2V) connected to DC amplifier and AD/

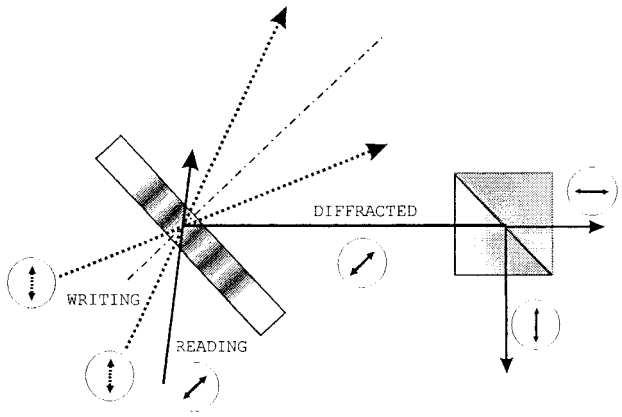

Figure 2. Optical scheme for rotational relaxation measurements. The polarizations of the writing (dotted lines), reading, and diffracted (solid lines) beams are indicated by encircled double arrows.

DA slot-card (Bitzer 03-9-45, with which the shutters were also operated) instead of more sophisticated photon counting instrumentation.

"Fast" Measurements. The writing part of the FRS setup corresponds to that used previously by the Mainz group[27,28] with beam diameters of ~0.5−2 mm, 60−100 mW laser light power, and 20−300 ms exposure time for hologram writing. The samples were in close contact with a brass sample holder using commercial regulation units to keep the temperature constant (better than 1 K). The writing beam could be blocked by a shutter (Melles Griot). For reconstruction, a He−Ne laser was used, whose beam was adjusted to the Bragg condition by two mirrors. The intensity of the diffracted beam could already be monitored during recording. Time resolution was approximately 20 ms, grating distances were within the limits of 0.6−20 μm. The exposure was chosen so that the diffraction efficiency did not exceed a few percent (which is still much higher than values usually achieved in FRS) and could thus be considered proportional to the square of the amplitude of refractive index modulation. In this case, the fit function for the experimentally measured intensity of diffracted light is $I(t) = \{A \exp[-(t/\tau_{tA})^{\beta_A}] - B \exp[-(t/\tau_{tB})^{\beta_B}]\}^2$.

Rotational Relaxation Measurements. During recording of a grating with linearly polarized light the dye molecules having their transition moment parallel to the electric vector of the light wave will preferably undergo phototransformation. This introduces a photoinduced orientational order which can decay by rotational diffusion of the dye molecules and their photoproducts.[14] The efficiency of light diffraction on such a grating depends on the polarization of the reconstruction beam. By monitoring the efficiency in different polarizations one obtains information on the time evolution of these rotational relaxation processes.[24] If we denote by $\Delta n_{||}$ and $\Delta n_{\perp}$ the index of refraction changes for parallel and perpendicular polarizations, respectively

$$R(t) = \frac{[\Delta n_{||}(t)/\Delta n_{\perp}(t)]}{[\Delta n_{||}(t)/\Delta n_{\perp}(t)]} \frac{\cos\theta - 1}{\cos\theta + 2} \qquad (1)$$

should be proportional to the rotational correlation function $\exp(-t/\tau_{rot})$ of the corresponding species. Here the factor $\cos\theta$ is the theoretical value[29] for $\Delta n_{\perp}/\Delta n_{||}$ in isotropic materials. In the case of PQ in PMMA rotation of at least two substantially different species must be taken into account, and the behavior is more complicated as will be discussed further below. $R(t)$ could be only considered as bearing the rotational information, without any translational contribution, in the limit of large grating periods, Λ.

For investigating rotational relaxation, the optical setup for "fast" measurements was supplied with two channel photodetection since $\Delta n_{||}$ and $\Delta n_{\perp}$ were measured simultaneously as follows (Figure 2). The polarization of the reading beam (λ = 633 nm) was slanted by an angle of $\cos^{-1}(3^{-1/2}) = 54.7°$ relative to that of the writing beam. The diffraction efficiency measured under this condition is not influenced by any rotational relaxation[24] (see Figure 9). To reveal the information on rotation, the reading beam diffracted from the grating was split with a polarizing beam splitter (Spindler & Hoyer, followed by two crystal polarizers), which separated the beam into two components with mutually perpendicular polarization (parallel and perpendicular to that of the writing beam; see

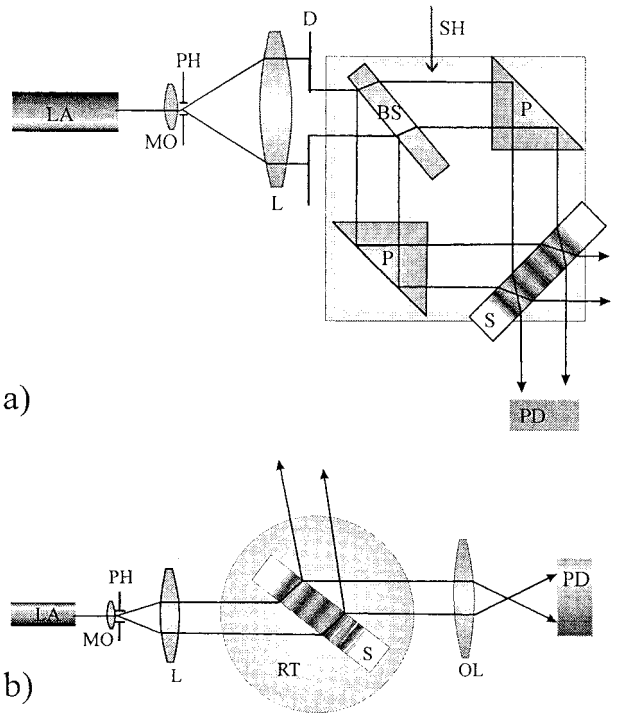

Figure 3. Optical schemes for "slow" measurements: separate setups for writing (a) and reconstructing (b) the gratings (see text for explanation of symbols).

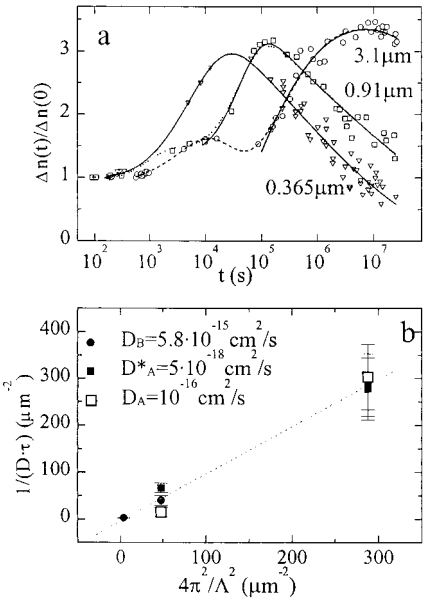

Figure 4. (a) Refractive index modulation $\Delta n(t)$ for grating with periods Λ = 0.365, 0.91, and 3.1 μm, recorded on phenanthrenequinone (PQ) in PMMA (M_w = 30 200). Solid lines represent fit with eq 3. (b) Demonstration of the grating growth due to diffusion of unbleached PQ ($D = D_B$, ●) and decay due to that of macromolecular photoproduct ($D = D_A$, calculated using fit-parameters τ, ■; or $D = D^*_A$, using averaged time constants $\langle\tau\rangle = \tau/\beta\Gamma(1/\beta)$, □). Temperature: 80 °C

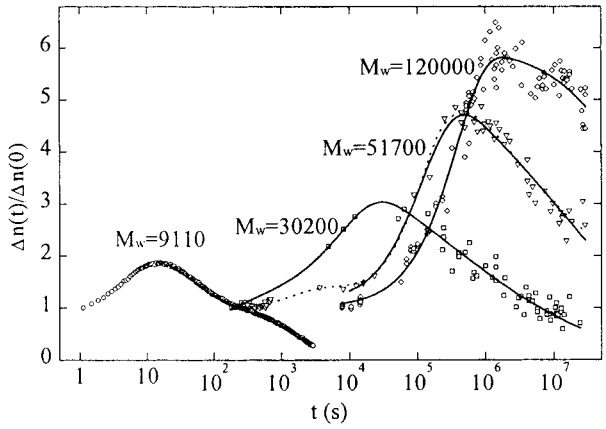

Figure 5. Refractive index modulation $\Delta n(t)$ for small grating spacing, $\Lambda = 0.365$ μm, in PMMA/PQ samples with different molar masses, M_w, at 80 °C. Solid lines represent fits with eq 3. Dashed line is the fit with four stretched exponentials.

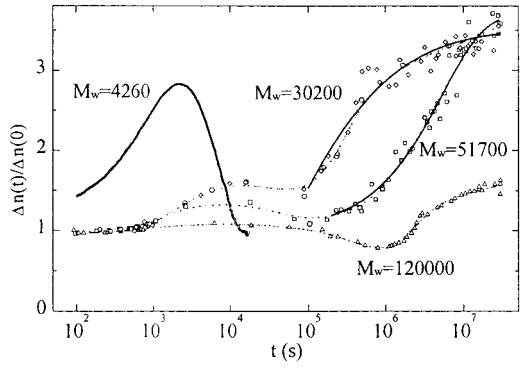

Figure 6. Refractive index modulation $\Delta n(t)$ for large grating spacing, $\Lambda = 3.1$ μm, in PMMA/PQ samples with different molar mass, M_w, at 80 °C. Solid lines represent fits with eq 3. Dashed lines are fits with more than two stretched exponentials.

Figure 2), which were then independently monitored by two photodiodes (see Figure 2). Prior to calculation of $R(t)$, the ratio of the two components $\Delta n_{||}$ and $\Delta n_{\perp}$ (measured in arbitrary units) must be normalized to $\Delta n_{\perp}/\Delta n_{||}(t \rightarrow \infty) = \cos\theta$, which is nearly one for small angles, θ (large Λ). To check for the complete orientational isotropy after times $t \gg \tau_A, \tau_B$ control measurements were also made using the setup described below which, however, revealed a long-lived optical anisotropy persisting over very long times (see Figure 10).

"Slow" Measurements. For long time experiments, we used a setup consisting of two separate parts, one (Figure 3a) for recording the hologram using an Ar^+ laser and a second (Figure 3b) for reconstruction of the phase hologram using a He−Ne laser. After the hologram was written at room temperature, the sample was placed in a thermostated oven and kept at the diffusion temperature for extended periods of time. To monitor the time evolution of the hologram efficiency, the sample was intermittently cooled to room temperature and adjusted on the reading table. The optical setup was similar to but not identical with that used in St. Petersburg.[10,12] The writing part is situated on an antivibration optical table. To ease finding and reconstruction of the gratings, the Ar^+ laser (LA) beam was expanded to a diameter of 20 mm. This was done with the help of a telescopic system consisting of a microscope objective (MO), a lens (L) with focal length $F =$ 150 mm, and a pinhole (PH) for spatial filtering. Only the central part of the beam (confined by the diaphragm D, diameter 5 mm) with relatively uniform intensity was used for writing the grating. Since light exposure could last as long as a few minutes the stability of the scheme during recording was improved by using several separate blocks—each consisting of a beam splitter (BS) and two prisms (P) or mirrors, with

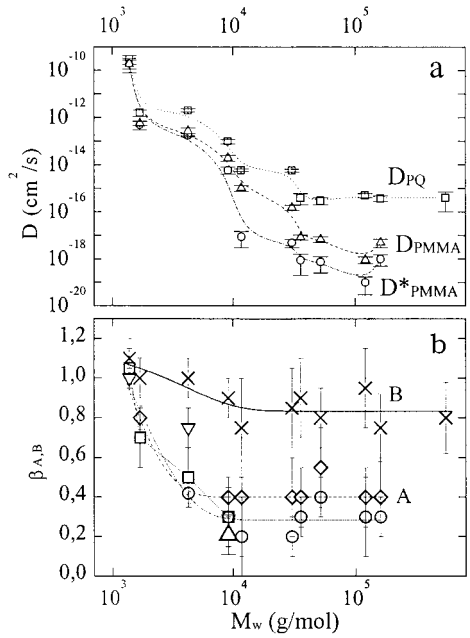

Figure 7. (a) Apparent "diffusion coefficients" (see text!) in PMMA/PQ samples at 80 °C drawn vs the molecular weight M_w. The D values were determined as slopes of $1/\tau$ plotted vs $4\pi^2/\Lambda^2$, where the characteristic times τ were stretched exponential fit-parameters for the experimental kinetics: D_{PQ} (□) for PQ diffusion from τ_B; D_{PMMA} (△) from τ_A; D^*_{PMMA} (○) from $\langle\tau_A\rangle$. (b) Stretching parameters β corresponding to D values in part a: β_A for the gratings with spatial periods 0.37 (○), 0.45 (△), 0.67 (□), 0.91 (◇), 6.7 μm (▽), and β_B, Λ-independent (×).

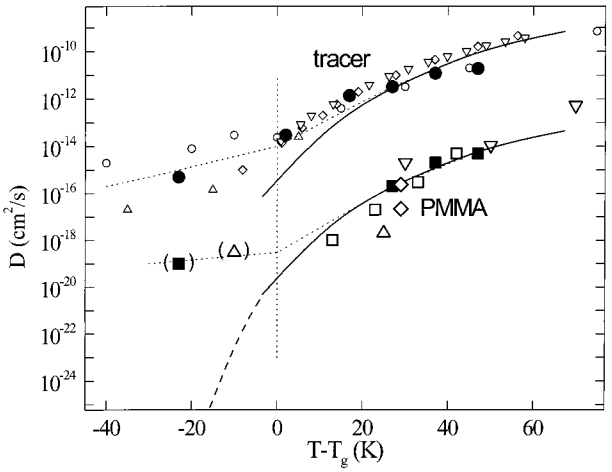

Figure 8. Diffusion coefficients of unbleached PQ (●) and polymer photoproduct (■) in PMMA (M_w =120 000) above and below T_g, in comparison with other data on tracer (camphoroquinone[33] (▽), tetrahydrothiophene−indigo[5] (◇), phenanthrenequinone[12,13] (○), and substituted anthracene[10] (△)) and macromolecular diffusion refs 12 (△), 22 (▽), 23 (□), and 32 (◇)). in PMMA. The full lines are shear relaxation time shift factors, a_T^{-1} (dashed line: WLF extrapolation), shifted in order to fit approximately the PQ and PMMA diffusion coefficients at the reference temperature, 403 K, of the shear relaxation experiments. The thin dotted lines are given just as guides for the eye. The symbols in brackets refer to polymer diffusion in the glass as discussed in the text.

fixed angles between the beams. The writing angles were chosen as $2\theta_{488\ nm} = 84$, 31, and 9°, respectively, corresponding to grating distances (spatial frequencies) of 0.365 (2740 mm^{-1}), 0.91 (1100 mm^{-1}), and 3.1 μm (320 mm^{-1}). In certain cases, writing the gratings in the nonlinear regime (concentration saturation) provided strong spatial harmonics of the grating being recorded, and they were reconstructed and monitored independently, as the gratings with multiple spatial frequen-

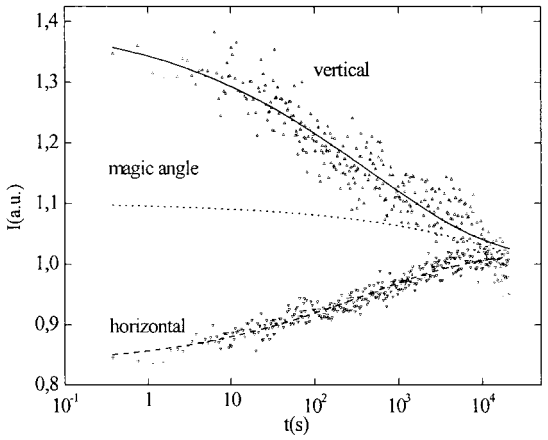

Figure 9. Rotational motion of Aberchrome-540 in PMMA (M_w = 120 000) at 80 °C. FRS intensity I, plotted vs time, for different polarizations of reconstructing light (λ = 633 nm): vertical (parallel to that of writing beams, solid line); horizontal (perpendicular, dashed line). The dotted line corresponding to polarization tilted by "magic angle" ($\cos^{-1}(3^{-1/2}) \approx 54.7°$), unaffected by rotation, is shown for reference.

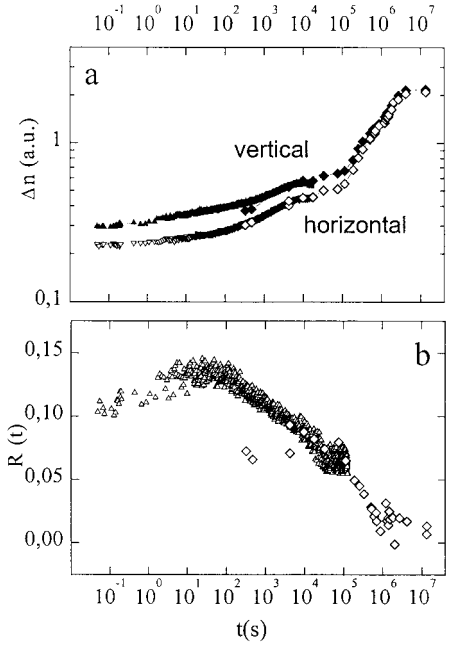

Figure 10. Rotational relaxation in PQ-doped PMMA (M_w = 30 200) at 80 °C: Refractive index modulation as a function of time, from diffraction efficiency measured in two polarizations perpendicular to that of writing beam: parallel (upper curve); perpendicular (lower curve). The data obtained with the "fast" setup (triangles) are matched with those of the "slow" setup (diamonds) at $t \sim 10^4$ s (see text). Rotational relaxation function $R(t)$ was evaluated via eq 1.

cies—640, 960, and 1280 mm^{-1} in addition to 320 mm^{-1}, and 2200 mm^{-1} in addition to 1100 mm^{-1}. Writing reflection holograms[14] by counterpropagating beams could in principle provide the highest spatial frequencies corresponding to $\Lambda \approx 0.16$ μm. But even an increase to $\Lambda \approx 0.22$ μm, which would be the smallest value still meeting the Bragg condition for both 488 and 633 nm, was not practicable with our long time experiments because reflection-type gratings are highly sensitive to effects such as shrinkage or swelling which could influence the sample thickness.

The writing process was monitored with the photodiode (PD) measuring the intensity of one of the writing beams behind the sample when one of the incident beams was temporarily blocked with a shutter (SH). Immediately after writing up to a relatively small diffraction efficiency of 3−5%, the sample was moved to the reconstruction setup for measurement of diffraction efficiency. The setup intended for measuring the diffraction efficiency (Figure 3b) consists of a He−Ne laser (LA), a telescopic system—a microscope objective (MO) with pinhole (PH) in focal point and a lens (L)—for beam expansion and spatial filtering, a rotatable table (RT) on which the sample (S) with the grating is installed and then rotated for Bragg angle tuning, and an objective lens (OL) which transfers the image of the grating to the plane of the photodiode (PD) supplied with an interference filter. The position of L was adjustable in order to allow for fitting of the curvature of the wave front to the grating geometry of the sample which could be distorted during long diffusion periods after exposure. Also OL could be moved to adjust the image of the grating to the input window of the photodiode. As the efficiencies of the gratings in these experiments were high enough (5−80%) to obtain the data on diffraction efficiency from the the intensity of the transmitted beam instead of that of the diffracted one, without loss of signal-to-noise ratio, we could take advantage of the linear beam geometry shown in Figure 3b and measure the intensity of the transmitted beam instead of that of the diffracted one, thus compensating for a possible change of the sample transparency. The minimum of transmitted light intensity (corresponding to maximum diffraction) was detected automatically while the angular position of the grating in the reading beam was scanned manually over the Bragg contour and then used for the calculations.

The refractive index modulation Δn is no longer proportional to the square root of the diffraction efficiency if the latter is larger than a few percent. It was therefore calculated as

$$\Delta n = C \sin^{-1}(1 - I_B/I_0)^{1/2} \qquad (2)$$

where I_0 is the photocurrent proportional to the intensity of the transmitted beam outside the Bragg contour (no light is diffracted by the grating), whereas I_B is the corresponding signal reduced by the diffracted intensity if Bragg's law is fulfilled, $C = (\lambda/\pi d)\cos\theta$ is a constant (λ, wavelength; Θ, incidence angle; d, material thickness) unimportant for our kinetic studies. By using this reconstruction setup, with Bragg angle adjustment performed each time, it was possible to perform measurements after diffusion periods up to several months, with no detectable perturbation in connection with setup stability. This setup was also used to check whether the diffraction efficiency of the gratings recorded in the setup for "fast" measurements was not too high, to be sure that the refractive index modulation could be still considered as proportional to the square root of diffraction efficiency.

The refractive index modulation, Δn, as determined via eq 2 was fitted by a superposition of stretched exponentials

$$\Delta n(t) = A \exp[-(t/\tau_{tA})^{\beta_A}] - B \exp[-(t/\tau_{tB})^{\beta_B}] \qquad (3)$$

in the time regime of the large maximum of Figures 4−6. The choice of a stretched exponential fitting function is for convenience and is not justified by theoretical considerations on the diffusion mechanism which is discussed further below. We also do not analyze the short time behavior of $\Delta n(t)$ characterized by a weak maximum or shoulder in Figures 4−6 and originating from a primary photoproduct reacting with the polymer to the final product which causes the long time decay.[12] Thus, the modulation amplitudes A and B are influenced by these reactions in addition to the bleaching reaction at $t = 0$. The decay times τ_{tA} and τ_{tB} should be related with the translational diffusion coefficients D_A and D_B of the polymer photoproduct and the unbleached PQ, respectively, by $\tau = \Lambda^2/(4\pi^2 D)$.

Results and Discussion

Translational Diffusion. In Figure 4, we have plotted the refractive index modulation $\Delta n(t)$ determined in PMMA (M_w = 30 200 with PQ tracer) at 80 °C for three different grating distances. A fit with eq 3

yields a stretching parameter of $\beta_B \gtrsim 0.9$ for the unbleached PQ. The corresponding decay time τ_{tB} is proportional to Λ^2 as is demonstrated by the plot in Figure 4b where the product $(D_B\tau_{tB})^{-1}$ is plotted vs $4\pi^2/\Lambda^2$ with $D_B = 5.8 \times 10^{-15}$ cm^2 s^{-1} being the average of the values obtained from the three fit curves in Figure 4a. The long time decay showed a larger stretching with parameters $\beta_A \lesssim 0.5$ which, however, could not be determined accurately because only part of the kinetics is available and the data points are broadly scattered (Figure 4a). The corresponding fits in other PMMA samples discussed below (Figure 7) indicate that β_A depends on the grating distance with values of $\approx$0.4 for $\Lambda = 0.91$ μm and $\lesssim$0.3 for $\Lambda = 0.365$ μm. After β_A was fixed to these values (0.4 and 0.3) the fit of the data in Figure 4a yields the grating diffusional lifetimes which are in turn used for obtaining the diffusion coefficient from the slope of plots $1/\tau$ vs $(2\pi/\Lambda)^2$. Though Figure 4b indicates that both τ_{tA}^{-1} and $\langle\tau_{tA}^{-1}\rangle$ (see below) are approximately proportional to Λ^{-2} one should note that the Λ dependence of β becomes apparent from separate straight lines through each data point and the origin. In Figures 5 and 6, the behavior of $\Delta n(t)$ is shown for some other PMMA samples of different molecular weights. It is remarkable that the long time decay can be followed and at least semiquantitatively evaluated even for high molecular weight samples with entangled PMMA chains at 80 °C well below the glass transition.

We should not discuss further the D values extracted from fits of $\Delta n(t)$ with eq 3 without considering before that in more detail the meaning of possible averages over the nonexponential decays. If we take the usual time average over a stretched exponential,[30] $\langle\tau_{tA}\rangle = \beta_A^{-1}\Gamma(\beta_A^{-1})\tau_{tA}$, with $\Gamma(...)$ being the gamma function, $\langle\tau_{tA}\rangle$ is the integral over the decay function and is thus dominated by contributions at long times. However, if we realize that the decay is related to displacements of the polymer photoproduct across the grating and we assume that the stretching is caused by spatial heterogeneity, we obtain an average over local diffusion coefficients in domains of which the system is assumed to be composed, namely, $\langle D\rangle = \sum w_i D_i$ with w_i being the fraction of domains "i" and D_i the corresponding local diffusion coefficient. Since $D \propto \tau^{-1}$, this average should be calculated from $\langle\tau_{tA}^{-1}\rangle$ rather than from $\langle\tau_{tA}\rangle$.[31] However, the short time behavior of the nonexponential decay function which is dominated by the rate average, $\langle\tau_{tA}^{-1}\rangle$, is not accessible from our experimental $\Delta n(t)$, which is influenced by the contribution from PQ diffusion and the enhanced polymer segmental motion that was already addressed in the Introduction. Thus, we should expect that the decay slows down as the displacements of the polymer photoproduct undergo the crossover from local segmental motion to center of mass motion of the polymer chain. This was investigated for the example of the lowest Δn(t) curve at $\Lambda = 0.365$ mm in Figure 4a. Here, we obtain $\beta_A = 0.5$ if only the data points for times $t < 10^{-6}$ s were fitted with eq 3. The inclusion of more data points at longer times results in a dramatic decrease of β_A down to 0.2 at $t = 3 \times 10^7$ s and a corresponding increase of the time average $\langle\tau_{tA}\rangle$ by a factor of 14 which reflects the crossover behavior of the diffusion process seen by the photoprobe attached to the polymer. In view of these complexities, we have decided to plot in Figure 7a two differently calculated *apparent* "diffusion coefficients" for comparison. The larger values are given by $D_A = \Lambda^2/(4\pi^2\tau_{tA})$ with the smallest Λ value indicated in Figure 7b and the τ_{tA} values obtained from the fit with eq 3. This provides a qualitative measure of the decay down to $\exp[-(t/\tau_{tA})^{\beta_A}] = e^{-1}$. The smaller values shown in Figure 7a are given by $D_A^* = \Lambda^2/(4\pi^2\langle\tau_{tA}\rangle)$ and should be considered as a rough measure of the long time behavior although we should note the limited time domain accessible for the largest molecular weights (see Figure 5). We should emphasize that the D_A values plotted in Figure 7a are rather different from the usual long time limits of Fickian center of mass diffusion shown in Figure 8 for polymer chain diffusion in the molten state. Nevertheless, we believe that our data provide important information on polymer chain motion below T_g (see below). The behavior of the stretching parameters shown in Figure 7b which decrease with decreasing Λ should be related by some kind of heterogeneity since Λ is much larger than the random chain dimensions, in particular, for shorter chains. On the other hand, we observe increased β_A values for the smaller molecular weights, $M_w \lesssim 5000$ and $\beta_B \gtrsim 0.8$ for the diffusion of unbleached PQ. The large β_B indicates that the diffusion of PQ averages over any spatial heterogeneity for displacements $(2Dt) \gtrsim 200$ nm. Finally, we should note that the weight average molecular weight, M_w, is the appropriate quantity for comparing different molecular weights since the photoproducts of PQ are distributed evenly over the polymer *segments* of the sample. M_n would be appropriate for polymers where each *chain* is labeled with one or a fixed number of dye molecules.

In Figure 8, we compare our results at 80 °C with diffusion coefficients obtained using the "fast" setup (see Experimental Section) in molten PMMA and with literature values. We have chosen the sample with $M_w = 120\,000$ and $M_w/M_n = 6$ which compares with the samples studied by Wang and Winnik[23] ($M_w \approx 145\,000$) and van Alsten and Lustig[22] ($M_w = 146\,000$ in matrix of $M_w = 88\,000$). Liu et al.[32] have obtained D values of 2.36×10^{-16} and 0.22×10^{-16} cm^2 s^{-1} for $M_w = 85\,500$ and 194 000, respectively, and $M_w/M_n \lesssim 1.05$.[32] Our polymer chain diffusion coefficients in PMMA melts are in fair agreement with those of the other workers. We have also compared in Figure 8 our PQ diffusion coefficients with those of other dye probes taken from the literature.[5,13,33] In view of the low accuracy attainable from the rising part of Δn(t) in our data, the agreement with the literature values is satisfactory and confirms our data analysis. Some results of previous diffusion measurements in the PMMA/PQ system shown in Figure 8 are also in harmony with the other data. Finally, we have included the temperature dependence of the shear relaxation time shift factor, a_T^{-1}, obtained from dynamical mechanical measurements in our PMMA sample ($M_w = 120\,000$).[34] It is apparent that any polymer diffusion coefficient estimated by extrapolation from the T dependence of a_T^{-1} would be many decades below the lowest number of $\sim 10^{-19}$ cm^2 s^{-1} obtained in our diffusion experiments at 80 °C.

Whereas the D values of dye tracer molecules below T_g are in harmony with the "falling out of equilibrium" seen in other relaxation experiments,[8] the huge enhancement of PQ−PMMA diffusion is rather unexpected. We have placed the corresponding two symbols in brackets in Figure 8 and discuss possible explanations further below. We note in passing that in dielectric relaxation experiments in polyisoprene melts a weaker T dependence was detected for the polymer chain than

for the segmental diffusion, which also indicates enhanced polymer chain diffusion if extrapolated below T_g.[35,36] However, the effect is relatively small and the Vogel temperature T_∞ predicted from WLF fits[8] is almost the same for both motional modes.[36]

Rotational Diffusion. The relaxation function, $R(t)$, defined in eq 1 provides information on reorientation processes from the index of refraction changes $\Delta n_{||}(t)$ and $\Delta n_\perp(t)$ determined as described in the Experimental Section. In the case of dye-labeled colloid spheres investigated previously,[24] $R(t)$ could be identified with the rotational correlation function of the spheres although the large stretching ($\beta \approx 0.45$) remained unexplained.

In the present case of PQ in PMMA, the situation is complicated by the fact that the translational diffusion already occurs on rather different time scales, and changes of $R(t)$ are observed over 8 decades in time (see below). Therefore, we have also studied the rotational diffusion of Aberchrome-540 (ACR)[37,38] where bleaching at $\lambda = 488$ nm results in a photoproduct which is not attached to the polymer, and the diffusion coefficient is of the same order as that of the initial compound since the FRS signal from ACR in low molecular weight glass formers above T_g develops in time perfectly exponentially.[38] $R(t)$ as determined from eq 1 can then be assumed to be proportional to the rotational correlation function. For solutions of 0.5% ACR in PMMA (M_w = 120 000) at 80 °C we have determined $\Delta n_{||}(t)$ and $\Delta n_\perp(t)$, shown in Figure 9, using a large grating distance, $\Lambda = 10\ \mu$m, which guarantees that the diffusional lifetime of the grating, $\Lambda^2/4\pi^2D$, is much longer than the rotational correlation time. This is confirmed by nearly constant $\Delta n(t)$ for the "magic angle" which eliminates the rotational contribution (see Figure 9). $R(t)$ as determined from eq 1 can then be assumed to be proportional to the rotational correlation function. By fitting $R(t)$ to a stretched exponential, $\exp[-(t/\tau_{rot})^{\beta_{rot}}]$, we obtained $\tau_{rot} = 340 \pm 60$ s, $\beta_{rot} = 0.30 \pm 0.03$, and thus an average rotational correlation time of $\langle\tau_{rot}\rangle = 3 \times 10^3$ s. These values are compatible with τ_{rot} and β_{rot} values of tetracene determined in polystyrene at $T_g - 10$ K by Ediger et al.[30]

In Figure 10a, we show values of $\Delta n_{||}(t)$ and $\Delta n_\perp(t)$ obtained for PQ in PMMA (M_w = 30 200) at 80 °C. We have used the "fast" and "slow" setups with $\Lambda = 7$ and 3.1 μm, respectively, to follow the depolarization behavior over a maximum time period. It should be noted that the absolute values of the hologram efficiency are measurable with the "slow" setup (see Experimental Section) which was used to match the values from the "fast" setup at $t \sim 10^4$ s.[39] Furthermore, we should realize that the overall increase of $\Delta n_{||}(t)$ and $\Delta n_\perp(t)$ with increasing time is due to translational diffusion (compare Figure 6 where this increase is shifted to smaller times for $\Lambda = 3.1\ \mu$m). Therefore, we cannot expect that $R(t)$ as determined from eq 1 and shown in Figure 10b has a simple relation with rotational diffusion. The initial rising part of $R(t)$ for $t < 10^2$ s is possibly related to the reorientational motions of the radicals resulting from the photoreaction, and the final polymer photoproduct might be responsible for the long time decay at $t > 10^5$ s. (It is remarkable that the anisotropy bleached into the PMMA sample by polarized light persists for many months at 80 °C. We refrain from speculating about explanations for this slow depolarization.) The main decay regime, 10^2 s $< t < 10^5$ s, should be attributed to rotational diffusion of unbleached PQ since this results in a rotational correlation time of $\sim 10^3$ s in agreement with that of ACR having about the same size (see Figure 11). From this coincidence, we felt encouraged to analyze corresponding results of $\Delta n_{||}$ and $\Delta n_\perp$ determined in the other PMMA samples using the "fast" setup in the same fashion. Thus, we fitted the curves by a superposition of two stretched exponentials [cf. eq 3] and attributed the long time decay to PQ reorientation. The corresponding τ_{rot} values are shown in Figure 11 along with *translational* correlation times, τ_{trans}, of PQ determined from the D values shown in Figure 7 via the mean square displacement

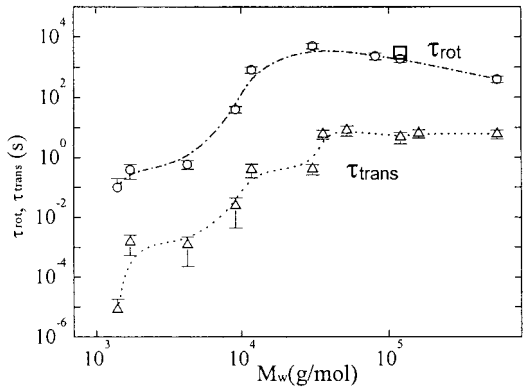

Figure 11. Characteristic times τ_{rot} (○) and τ_{trans} (△) for rotational and translational diffusion of phenanthrenequinone in PMMA at 80 °C, drawn vs the molecular weight. The Aberchrome-540 value of τ_{rot} (□) is also shown for comparison. Lines are guides to the eye.

$$\langle r^2\rangle = 6D\tau_{trans} \qquad (4)$$

where we have chosen $\langle r^2\rangle^{1/2} = 0.7$ nm which is the size of the PQ molecule estimated from its molar volume. It is apparent from the difference between τ_{rot} and τ_{trans} that large displacements of ~20 times the molecular size are obtained if τ_{trans} is replaced by τ_{rot} in eq 4 This demonstrates the translational enhancement that was also found, e.g., for tetracene tracers in polystyrene at $T \sim T_g$.[6] It is also noteworthy that τ_{rot} and τ_{trans} are approximately independent of M_w in the regime $M_w \gtrsim 10^4$ whereas the values decrease in the oligomer regime due to the smaller T_g values.

Aging Effects and Heterogeneity. A rather peculiar feature of our diffusion experiments, which is most pronounced at molecular weights $M_w \lesssim 10\,000$ is the large influence of aging effects demonstrated in Figure 12 for sample 3 with $M_w = 4260$ and $T_g = 96$ °C. Here the first $\Delta n(t)$ curve was determined within a few hours after cooling from the melt to 80 °C. The second curve was obtained after annealing at 80 °C for 2 months. Whereas the rising portion due to PQ diffusion was hardly changed the decay was stretched to longer times and exhibited a shoulder at $t \sim 3000$ s shifted by almost two decades from the maximum at ~50 s. This looks as if a certain fraction of the chains is pinned down for increasing periods of time during the process of physical aging. Unfortunately, this phenomenon is very difficult to study in a systematic way with reproducible results, and the aging times increase with increasing molecular weight. Thus, we believe that the diffusion coefficients for $M_w \gtrsim 10\,000$ are not sizeably affected by this particular kind of aging. However, we cannot be sure whether the slowing of the decay at very long times

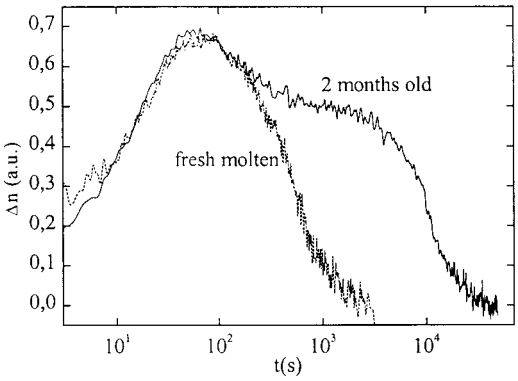

Figure 12. Effect of polymer aging on development of the FRS grating. The two experimental curves show the refractive index modulation Δn (grating distance, $\Lambda = 0.67\ \mu$m) as a function of time, determined in the same PMMA/PQ sample (M_w = 4260) within a few hours after melting (dotted line) and after annealing at 80 °C for two months (solid line).

discussed in relation with the $\Lambda = 0.365\ \mu$m curve in Figure 4a is partly due to aging effects (see below).[40] Physical aging in PMMA has been studied previously by calorimetry,[41,42] mechanical relaxation,[43,44] and other techniques.[30,45−47] In polystyrene, the rotational diffusion of rubrene tracers showed a large slowing on aging at $T_g - 10$ K.[30,47]

The large translational enhancement of PQ diffusion exhibited in Figure 11 (see above) can be explained by the influence of dynamical heterogeneity which has also been observed in other polymers and glass-forming liquids close to the glass transition.[6,31,48,49] This means that the PQ molecules may undergo large displacements if they are in a mobilized domain but may be almost fixed if they are packed within an immobilized environment.[6,31,48]

The influence of dynamic heterogeneities upon chain diffusion is more complex. Although, the center of mass will already be displaced if only part of the chain moves in a *mobilized state* one should expect that center of mass displacements over large distances (≳100 nm) will be very slow, and they are only possible if the lifetime in *immobilized states* is much smaller than the time of the corresponding diffusion experiment. Let us illustrate this point by considering the FRS long time decay for the PMMA sample 8 (M_w = 51 700, T_g = 104 °C) in Figure 5. After the diffusion time of $t = 3 \times 10^7$ s (350 days), the long time decay is at about half of its maximum value, and we have thus

$$\Delta n(t)/\Delta n(0) = \exp[-(2\pi/\Lambda)^2\langle r(t)^2\rangle/6] \approx 1/2 \qquad (5)$$

which yields the rms displacement $\langle r(t)^2\rangle^{1/2} \approx 120$ nm, for $\Lambda = 365$ nm, if the Gaussian approximation is justified. Since the size of the PMMA random chains of ∼500 monomer units is about 20 nm (somewhat larger than the end-to-end distance), it appears plausible to assume a similar size for the mobilized regions in order to rationalize the possibility of ∼120 nm displacements within a finite time. This estimate is in harmony with the size of "perhaps 10 nm" obtained by Ediger and coworkers from the translational enhancement of tetracene tracers in polystyrene at the glass transition.[48] The situation should be similar for our PMMA sample 9 (M_w = 120 000, M_n = 20 000) where the displacement is smaller (see Figure 5) and probably mostly due to the short chains within the very broad molecular weight distribution. Here, the glass transition region is also rather broad in the DSC curves recorded for obtaining the T_g values of Table 1. It has been found[43] that the glass transition region is particularly broad in PMMA samples with comparable amounts of syndiotactic (st) and isotactic (it) triads because of the large difference in the T_g values (45 °C in it-PMMA and 130 °C in st-PMMA) and the possible complex formation between both species. In blends of it- and st-PMMA the glass transition was found to extend over more than 50 K without development of two separate regions.[43] Since the authors report thermally induced crystallization under certain conditions,[43] we have checked two of our samples (nos. 2 and 4) where large aging effects were observed by X-ray scattering; however, no indications of crystal formation could be seen.[51] Nevertheless, we should not exclude the possibility that aging effects which have been observed in PMMA down to room temperature[44] are related with the long time behavior of our results (Figure 5). This may also be suggested by recent "thermally stimulated current thermal sampling" experiments in PMMA samples of varying content of iso- and syndiotactic triads.[52] The authors conclude that the presence of low T_g "pockets" of predominantly isotactic sequences contributes to the broad glass transition and that their cooperative motion may be the origin of low-temperature aging phenomena.[52] Although they had in mind length scales of only a few nanometers we may speculate further that the aging of the *nonequilibrium* state obtained by cooling PMMA to 80 °C involves long time cooperative motion of larger regions (∼20 nm), perhaps caused by spurious stress components, and this internal rearrangement causes the large displacement of the PQ−PMMA photoproduct molecules over large distances of ≳100 nm as estimated above. Though this is only a vague speculation it may provide an alternative to the assumption that a single polymer molecule can undergo diffusional displacement by more than 5 times its random coil size at $T_g - 24$ K (as discussed above for sample 8), which is hard to accept even if the diffusion time is 1 year.

In view of the above speculations, one may question the significance of our results. Here it is noteworthy to consider the data in Figure 4a and Figure 5 at the longest times of $\sim 10^7$ s. The *differences* seen at small and large grating distances, Λ, as well as at small and large M_w can certainly not be explained by chemical processes nor by chain degradation, in particular, since we have found no reduction of M_w after the annealing period. Since large scale convectional flow can be excluded in view of the Λ^2 dependence (Figure 4) the possibility of diffusional displacement should be seriously considered. Thus we hope our results will stimulate further research.

In future experiments the complex aging behavior of PMMA originating in part from the large T_g difference between it- and st-PMMA should be avoided. Here, polystyrene (PS) would be preferable since it- and st-PS have nearly the same T_g and the aging behavior of atactic PS is well-known down to $T_g - 10$ K.[47] Since the rise and decay behavior of the FRS curves in the PQ/PMMA system, due to the counter phase gratings of monomer dye and polymer photoproduct, masks the early stages of chain diffusion a system should be preferable where the diffusion of monomer tracers and labeled polymers can be studied in separate samples. So far, we have no dye label that binds covalently to PS and yields sufficient hologram efficiency for applica-

tion of our "slow" setup(Figure 3). We hope that appropriate dye labeled polymers will be available in the future. A further possibility to look for polymer chain displacement is the neutron reflection technique which has been applied to investigate the initial stages of PMMA and PS diffusion across the interface between films of the respective protonated and deuterated species at $T > T_g$.[53,54] Although only displacements up to about 10 nm are accessible by this technique it would provide an excellent test of whether chain interpenetration below the glass transition occurs at all after very long annealing times, and it should contain information on the displacement mechanism if it occurs. Other techniques that monitor the interdiffusion of protonated and deuterated polymers across an interface (e.g., forward recoil scattering[55]) have a lower spatial resolution and will thus require longer annealing times. However, they should provide clear evidence on whether the interpretation of our results can be substantiated or we must look for alternative explanations.

Conclusions

In a first study of polymer chain diffusion below the glass transition, we have found strong indications for large center of mass displacements of PMMA chains at temperatures of more than 20 K below T_g. Although, no real long time diffusion coefficients could be determined, our estimates indicate that PMMA molecules, e.g., in a sample of $M_w = 51\,700$ and $T_g = 104$ °C are displaced by at least ~120 nm during an annealing time of 350 days at 80 °C. This signifies a translational enhancement by many decades over estimates from the T-dependence of shear viscosity which would predict unmeasurably small D values below 10^{-28} cm^2 s^{-1} for this case (see Figure 8). For a possible explanation, we suggest that dynamical heterogeneities with mobile regions of up to ~20 nm exist in this temperature range and that the corresponding immobilized regions have lifetimes far below typical diffusion times. An alternative, more speculative, interpretation assumes that the large displacements are related with long time aging effects that may involve cooperative motion of large regions (~20 nm), perhaps caused by spurious stress components, over the large distances (> 100 nm) detected in our experiments. Although it is known from calorimetric as well as thermal and mechanical relaxation experiments that molecular mobility (e.g., redistribution of free volume) is possible down to about 50 K below T_g,[41−44,52,56] the large displacements indicated by our FRS results are rather unexpected and should be investigated by further experiments, in particular, by the neutron reflection technique where chain interdiffusion across an interface can be detected with high spatial resolution up to distances of about 10 nm.[53]

With a particular FRS setup that allows for studies of translational and rotational diffusion with experimental times of many months, we have also determined translational and rotational diffusion coefficients of dye tracers and we have observed a small but distinct orientational anisotropy that persists in PMMA at 80 °C for times up to 1 year.

Acknowledgment. We wish to thank Prof. Dr. A. H. E. Müller and co-workers for providing and characterizing the PMMA samples, Prof. Dr. T. Pakula for the dynamic mechanical and DSC measurements, Dr. J. Spickermann for MALDI−TOF measurements, and Dr. M. Stamm for the X-ray scattering experiments and for helpful discussions. A.V. is grateful to the A. v. Humboldt Foundation for a fellowship. Support by the Deutsche Forschungsgemeinschaft (SFB 262) and the Fonds der Chemischen Industrie is gratefully acknowledged.

References and Notes

(1) Lodge, T. P.; Rotstein, N. A.; Prager, S. *Adv. Chem. Phys.* **1990**, *79*, 1.
(2) Binder, K.; Sillescu, H.; In *Encyclopedia of Polymer Science and Engineering, Supplement*, 2nd ed.; Mark, Bikales, Overberger, and Menges, Eds.; Wiley: New York, 1989; pp 297−315.
(3) Doi, M.; Edwards, S. F. *The Theory of Polymer Dynamics*; Clarendon Press: Oxford, England, 1986.
(4) Schweizer, K. *J. Chem. Phys.* **1989**, *91*, 5802.
(5) Ehlich, D.; Sillescu, H. *Macromolecules* **1990**, *23*, 1600.
(6) Cicerone, M. T.; Ediger, M. D. J. *Chem. Phys.* **1996**, *104*, 7210.
(7) Veniaminov, A. V.; Burunkova, Yu. E.; Kazannikova, A. V. *Int. Polym. Sci. Technol.* **1989**, *16*, 109.
(8) Ferry, J. D. *Viscoelastic Properties of Polymers*, 3rd. ed.; Wiley: New York, 1980.
(9) Green, P. F.; Kramer, E. J. *Macromolecules* **1986**, *19*, 1108 and references therein.
(10) Veniaminov, A. V.; Lashkov, G. I.; Ratner, O. B.; Shelekhov, N. S.; Bandyuk, O. V. *Opt. Spectrosc.* **1986**, *60*, 87.
(11) Veniaminov, A. V.; Goncharov, V. F.; Popov, A. P. *Opt. Spectrosc.* **1991**,*70*, 505.
(12) Veniaminov, A. V.; Sedunov, Yu. N.; Popov, A. P.; Bandyuk, O. V. *Opt. Spectrosc.* **1996**, *81*, 617.
(13) Veniaminov, A. V.; Sedunov, Yu. N. *Polym. Sci.* **1996**, *38*, 71.
(14) Eichler, H. J.; Günter, P.; Pohl, D. W. *Laser-induced dynamic gratings*; Springer: Berlin, 1986.
(15) Bruce, J. M. *The chemistry of the quinoid compounds, Part 1*; Wiley: New York, 1974.
(16) Carapellucci, P. A.; Wolf, H. P.; Weiss, K. *J. Am. Chem. Soc.* **1969**, *91*, 4635.
(17) Bandyuk, O. V.; Shelekhov, N. S.; Popov, A. P.; Danilova, M. Ya. *J. Appl. Chem. USSR.* **1988**, *61*, 946.
(18) Spickermann, J. Private communication.
(19) Freilich, Y. L.; Levy, M.; Reich, S. *J. Polym. Sci.: Polym. Chem. Ed.* **1977**, *15*, 1811.
(20) Park, S.; Sung, J.; Kim, H. *J. Phys. Chem.* **1991**, *95*, 7121.
(21) Zhang, J.; Wang, C. H. *J. Phys. Chem.* **1986**, *90*, 2296.
(22) van Alsten, J. G.; Lustig, S. R. *Macromolecules* **1992**, *25*, 5069.
(23) Wang, Y.; Winnik, M. A. *Macromolecules* **1993**, *26*, 3147.
(24) Kanetakis, J.; Sillescu. H. *Chem. Phys. Lett.* **1996**, *252*, 127.
(25) Mai, P. M.; Müller, A. H. E. *Macromol. Chem., Rapid Commun.* **1987**, *8*, 99; Kraft, R.; Müller, A. H. E.; Warzelhan, V.; Höcker, H.; Schulz, G. V. *Macromolecules* **1978**, *11*, 1095.
(26) Matveev, Yu. I.; Askadskii, A. A. *Polym. Sci., Ser. A* **1993**, *35*, 50.
(27) Antonietti, M.; Coutandin, J.; Grütter, R.; Sillescu, H. *Macromolecules* **1984**, *17*, 798.
(28) Sillescu, H.; Ehlich, D. In: *Lasers in Polymer Science and Technology, Applications*; V. III., Fouassier, J.-P.; Rabek, J. F., Eds.; CRC Press: Boca Raton, FL, 1990; Vol. V.III., pp 211−226.
(29) Kogelnik, H. *Bell Syst. Tech. J.* **1969**, *48*, 2909.
(30) Inoue, T.; Cicerone, M. T.; Ediger, M. D. *Macromolecules* **1995**, *28*, 4325.
(31) Chang, I.; Sillescu, H. *J. Phys. Chem. B* **1997**, *101*, 8794.
(32) Liu, Y.; Reiter, G.; Kunz, K.; Stamm, M. *Macromolecules* **1993**, *26*, 2134.
(33) Zhang, J.; Wang, C. H.; Ehlich, D. *Macromolecules* **1986**, *19*, 1390.
(34) Pakula, T. Private communication.
(35) Adachi, K.; Kotaka, T. *Macromolecules* **1985**, *18*, 466.
(36) Boese, D.; Kremer, F. *Macromolecules* **1990**, *23*, 829.
(37) Kardinahl, T.; Franke, H. *Appl. Phys. A, Mater. Sci., Proc.* **1995**, *61*, 23.
(38) Heuberger, G.; Sillescu, H. *J. Phys. Chem.* **1996**, *100*, 15255.
(39) The reduced $\Delta n_{||}$ values obtained with the "slow" setup at $t \approx 300$ s are probably due to an artifact; this deviation causes substantial errors in the calculated values of R, because $\Delta n_{||} - \Delta n_{\perp} \ll \Delta n_{||}$ (see also scattered points $R(t)$ at long times, where $\Delta n_{||} \approx \Delta n_{\perp}$).
(40) However, no noticeable difference was found in DSC made before and after the course of FRS measurements

(41) Hodge, I. M. *Macromolecules* **1987**, *20*, 2897.
(42) Frühauf, K.-P.; Helwig, J.; Müser, H. E.; Krüger, J. K.; Roberts, R. *Colloid Polym. Sci.* **1988**, *266*, 814.
(43) Allen, P. E. M.; Host, D. M.; Van Tan Truong; Williams, D. R. G. *Eur. Polym. J.* **1985**, *21*, 603.
(44) Muzeau, E.; Cavaille, J. Y.; Vassoille, R.; Prez, J.; Johari, G. P. *Macromolecules* **1992**, *25*, 5108.
(45) Curro, J. J.; Roe, R.-J. *Polymer* **1984**, *25*, 1424.
(46) Royal, J. S.; Torkelson, J. M. *Macromolecules* **1993**, *26*, 5331.
(47) Ediger, M. D.; Inoue, T.; Cicerone, M. T.; Blackburn, F. R. *Macromol. Chem. Phys., Macromol. Symp.* **1996**, *101*, 139 and references therein.
(48) Cicerone, M. T.; Blackburn, F. R.; Ediger, M. D. *Macromolecules* **1995**, *28*, 8224.
(49) Böhmer, R.; Chamberlin, R. V.; Diezemann, G.; Geil, B.; Heuer, A.; Hinze, G.; Kuebler, S. C.; Richert, R.; Schiener, B.; Sillescu, H.; Spiess, H. W.; Tracht, U.; Wilhelm, M. *J. Non-Cryst. Solids* **1998**, *235−237*, 121.
(50) Non-Gaussian effects are apparent from the small and Λ-dependent stretching β shown in Figure 7b. However, even the low D value of 10^{-18} cm^2 s^{-1} given in Figure 7a for sample 8 yields $(6Dt)^{1/2} = 134$ nm, which is larger than the estimate of 120 nm from eq 5.
(51) Stamm, M. Private communication.
(52) Sauer, B.B.; Kim, Y. H. *Macromolecules* **1997**, *30*, 3323.
(53) Kunz, K.; Stamm, M. *Macromolecules* **1996**, *29*, 2548.
(54) Kuhlmann, T.; Kraus, J.; Müller-Buschbaum, P.; Schubert, D. W.; Stamm, M. *J. Non-Cryst. Solids* **1998**, *235−237*, 457.
(55) Tead, S. F.; Kramer, E. J. *Macromolecules* **1988**, *21*, 1513.
(56) Hodge, I. M. *J. Non-Cryst. Solids* **1994**, *169*, 211.

MA981312D